A Rationale for the Preparation of Asymmetric Pervaporation Membranes*

M. H. V. MULDER, J. OUDE HENDRIKMAN, J. G. WIJMANS, and C. A. SMOLDERS, *Department of Chemical Technology, Twente University of Technology, P.O. Box 217, 7500 AE Enschede, The Netherlands*

Synopsis

Pervaporation is carried out primarily with homogeneous membranes. An improvement in permeation rate can be achieved by using asymmetric or composite membranes. In order to maintain a high selectivity, very dense top layers are needed. The formation of asymmetric pervaporation membranes will be discussed in terms of the model proposed by our group: formation of the top layer by gelation; formation of the porous sublayer by liquid–liquid phase separation followed by gelation of the concentrated polymer phase. To obtain very dense top layers the following factors are important: the ratio of nonsolvent inflow and solvent outflow, polymer concentration, location of the liquid–liquid demixing gap, and location of the gel region. Asymmetric membranes have been prepared by varying these factors, and the obtained membranes have been tested on ethanol/water mixtures.

INTRODUCTION

Despite intensive investigations of Binning and co-workers[1-3] in the late fifties and early sixties, the commercial applications of pervaporation as membrane separation process are still very limited. There are three main reasons for this: (i) The energy consumption is relatively high compared to other membrane processes such as ultrafiltration and hyperfiltration because a phase transition occurs and the heat of vaporization has to be supplied; (ii) insufficient permeation rates and/or insufficient selectivities; (iii) process design is difficult because of a temperature drop across the membrane and pressure losses at the downstream side. Nevertheless, there are several interesting potential applications such as the removal of water from organic liquids, the removal of organic contaminants (e.g., aromatics and chlorinated hydrocarbons) from waste water and the separation of some azeotropic and isomeric mixtures. In the last decade much attention has been paid to the separation of ethanol/water mixtures,[4-9] and recently a commercial application was described for the production of ethanol from biomass using pervaporation for the final dehydration step.[10]

The separation mechanism of pervaporation is a solution–diffusion mechanism[11-14] because very dense membranes are needed. Till now pervaporation is carried out primarily with dense homogeneous membranes. Only incidentally the use of asymmetric membranes has been reported,[5,15]

* A part of this paper was presented at the Europe-Japan Congress on Membranes and Membrane processes, June 18–22, 1984, Stresa/Italy.

Journal of Applied Polymer Science, Vol. 30, 2805–2820 (1985)
 CCC 0021-8995/85/072805-16$04.00

and no systematic investigations have been performed to obtain asymmetric pervaporation membranes.

As already mentioned above, one of the disadvantages of the pervaporation process are the low permeation rates especially with highly selective membranes. The permeation rate through a homogeneous membrane is roughly inversely proportional to membrane thickness. One way to reduce the effective membrane thickness is to prepare asymmetric membranes.

Loeb and Sourirajan[16] were the first to prepare asymmetric hyperfiltration membranes. Since their work much research has been carried out on the development of new and better asymmetric membranes, often rather empirically and sometimes by a more fundamental approach. In our laboratory much attention has been paid to the fundamental approach.[17-25] Asymmetric membranes are produced by phase inversion.[26] The concept of phase inversion covers a range of different techniques,[25] and in this paper we will discuss the preparation of asymmetric membranes by immersion precipitation. Immersion precipitation is the most widely used technique for preparing asymmetric membranes: A polymer solution is cast on a suitable support and immersed in a nonsolvent coagulation bath. The asymmetric membrane is formed by exchange of solvent and nonsolvent. The ultimate membrane structure is determined by the thermodynamics and kinetics of the demixing process, a.o., by the choice of the system polymer/solvent/nonsolvent. Sometimes a curing step can improve membrane performance.

When asymmetric membranes are used in pervaporation experiments there are two possibilities of installing the membrane: the top layer is facing the feed ("skin up"); the porous sublayer is facing the feed ("skin down"). The influence of the porous sublayer on mass transfer should not be neglected. In the case of "skin up" position the resistance at the feed/membrane interface is equal to that for the homogenous membranes but the resistance in the porous layer can be appreciable when high vacuum is applied downstream, especially when the pore diameter is small and the permeation rate is high. In the case of "skin down" position the porous sublayer acts as a stagnant layer and the extent of concentration polarization will strongly depend on the structure of the porous sublayer; this effect increases with increasing permeation rates. Therefore, in developing asymmetric membranes the pores in the sublayer should be as large as possible.

The objective of this paper is to discuss the preparation of asymmetric membranes with a very dense top layer prepared from various polymers and to discuss the different factors to obtain these dense top layers.

THEORETICAL CONSIDERATIONS

In our group the hypothesis has been adopted that two distinctly different types of phase separation processes are responsible for the formation of asymmetric membranes[17-25]: gelation (or crystallization) for the formation of the top layer; liquid–liquid phase separation followed by gelation of the concentrated polymer phase for the formation of the porous sublayer. Koenhen et al.[17] were the first who suggested this mechanism. In this paper we

will describe the formation of asymmetric pervaporation membranes with a very dense top layer in terms of this mechanism.

Some polymers have no ability to crystallize; in that case the mechanism of crystallization for the formation of the top layer can be excluded. For these amorphous polymers there is no liquid–solid phase transition in the thermodynamic sense and gelation generally occurs by entanglement or by physical interactions between segments. The more numerous the entanglements, the more dense the gel will be. This is also the reason why homogeneous membranes are very suitable for pervaporation. Homogeneous membranes are prepared by evaporation of the solvent from a polymer solution film. During evaporation the polymer concentration increases, the viscosity increases, and the chains become more and more immobile, reaching a very high packing density when all the solvent has been evaporated. When asymmetric pervaporation membranes are developed the top layer should at least have the same dense structure as that for the homogeneous membranes obtained by complete evaporation.

Liquid–Liquid Phase Separation

Liquid–liquid phase separation occurs if a system can lower its free enthalpy of mixing by separating into two liquid phases. Generally, membrane forming systems are ternary systems consisting of a polymer, a solvent, and a nonsolvent. Figure 1 shows a schematic diagram of a ΔG_m surface for a ternary system. All pairs of composition with a common tangent plane to the ΔG_m surface constitute the solid line at the bottom of the phase diagram. This line is called the binodal. The dotted line which connects the points of inflection is called the spinodal. In the critical point (C_r) the binodal and spinodal touch each other. The location of the critical point determines whether the nuclei formed at a certain point when the binodal is crossed

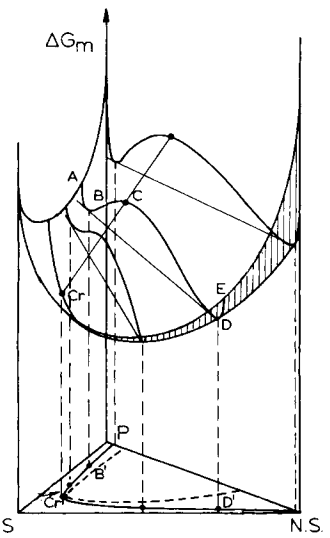

Fig. 1. Sketch of the ΔG_m surface and miscibility gap for the system polymer (P), solvent (S), and nonsolvent (NS); Cr = critical point.

will have a composition high or low in polymer concentration. If the binodal is entered between point C_r' and P, demixing occurs if nuclei of the second phase (the dilute polymer phase) are generated. After nucleation, these droplets will grow further until the surrounding polymer-rich phase will have such a high polymer concentration that gelation occurs.

Figure 1 shows a liquid–liquid demixing gap only. In Figure 2 a ternary phase diagram is shown where, except for the binodal demixing gap, a gel region (arbitrarily chosen) has also been drawn. The exact location of this gel region is difficult to establish. In fact, there is no fixed location because kinetic factors such as rate of solvent outflow and nonsolvent inflow will influence the exact location. The boundary of this gel region is more or less a viscosity boundary, and the effect of increasing viscosity on phase separation and membrane structure has to be considered.

Structure formation in asymmetric membranes reflects strongly different time regimes for composition changes at different positions in the coagulating film: directly below the interface coagulation bath/cast polymer solution the top layer is being formed during rapid solvent loss; at greater depth below the interface the sublayer structure is being formed during a more or less gradual exchange of solvent and nonsolvent. These different composition changes for top layer and sublayer have earlier been described and visualized in the ternary phase diagram as "composition path."[22,27] For top layer formation there are two possibilities: (i) the coagulation path crosses the gel region before intersecting the binodal demixing gap (Fig. 2, arrow AC) or (ii) the coagulation path intersects the binodal first (Fig. 2, arrow AB). In the first case the gel region is entered at point C, in a part of the phase diagram where the three components are still completely miscible with each other (one-phase region). Now suppose that upon entering the gel region the polymer chains would be immobilized completely. In that case the polymeric structure has been fixed. However, the diffusion will go on, and there will be a complete exchange of solvent and nonsolvent. In this hypothetical case the polymer–nonsolvent axis will be reached at point D. If during gelation further shrinkage of the gel volume, i.e., syneresis occurs,[20] it is possible that the polymer–nonsolvent axis is reached at higher polymer concentrations (point E). Syneresis will occur if the system can decrease its free enthalpy of mixing because the polymer molecules can

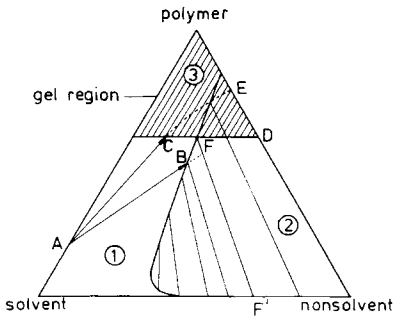

Fig. 2. Schematic phase diagram for a ternary system with a one-phase region (①), a two-phase region (②), and a gel region (③). For further explanation of coagulation paths, see text.

change to a less expanded conformation involving loss of solvent (and nonsolvent).

In the second case when the coagulation path intersects the binodal at lower polymer concentrations (Fig. 2, arrow AB), one of the two demixed phases which are in equilibrium with each other (the polymer rich phase) will reach the gel region after a certain time at point F. The same will happen with this phase as mentioned above; the polymer concentration will not increase much because of the immobility of the chains and further growth of the diluted phase is impeded. Again the mechanism of syneresis should not be excluded. Research on this topic (location of the gel region and syneresis) is carried out in our laboratory, and the results will be published in the near future.

Membrane formation is a dynamic process, thermodynamics alone cannot describe the process fully, also kinetics should be included, i.e., rates of solvent outflow and nonsolvent inflow, kinetics of gelation and kinetics of nucleation, and growth during liquid–liquid demixing. Nevertheless, we will demonstrate that the thermodynamic considerations provide a good indication how to obtain a more dense top layer.

Formation of the Top Layer

According to the Flory–Huggins theory[28] the free energy of mixing (ΔG_m) for a ternary system is given by

$$\frac{\Delta G_m}{RT} = n_1 \ln \phi_1 + n_2 \ln \phi_2 + n_3 \ln \phi_3 + g_{12}(u_2) n_1 \phi_2 + \chi_{13} n_1 \phi_3 + \chi_{23} n_2 \phi_3 \tag{1}$$

The subscripts refer to nonsolvent (1), solvent (2), and polymer (3). n_i and ϕ_i are the number of moles and the volume fraction, respectively. χ_{13} is the nonsolvent–polymer interaction parameter, and χ_{23} the solvent–polymer interaction parameter. Both parameters are assumed to be concentration-independent. g_{12} is the solvent–nonsolvent interaction parameter, and this parameter is assumed to be a function of u_2, with $u_2 = \phi_2/(\phi_1 + \phi_2)$ in the notation of Živný and Pouchlý.[29]

Different factors are very important for the formation of the top layer: the ratio of nonsolvent inflow (J_1) and solvent outflow (J_2); polymer concentration, in the casting solution; location of the liquid–liquid demixing gap; location of the gel region. Figure 3 gives a schematic representation of the film/bath interface. The ratio of the solvent outflow (J_2) and nonsolvent inflow (J_1) determines the course of the coagulation path. In order to obtain a dense top layer, the ratio J_1/J_2 should be small, and the coagulation path will reach the gel region before intersecting the binodal. J_1 and J_2 can be represented by a simplified phenomenological relation

$$J_i = L_i(\phi_i, v_i)\Delta\mu_i \tag{2}$$

$\Delta\mu_i$, the chemical potential difference, is the driving force for mass transport of component i through the film/bath interface (see Fig. 3) and L_i is the

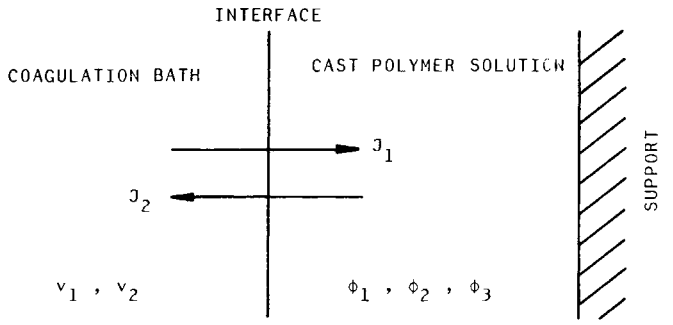

Fig. 3. Fluxes of nonsolvent (J_1) and solvent (J_2) at the interface coagulation bath/cast polymer solution. Components: (1) solvent; (2) nonsolvent; (3) polymer.

permeability coefficient of component i which may be a function of ϕ_i and v_i. Calculations performed by Altena[30] showed that in the early stage of membrane formation the ratio of J_1/J_2 is very small and, consequently, a very steep coagulation path results which intersects the gel region at low nonsolvent content (see Fig. 2, arrow AC). If we disregard the influence of L_i (or assume the ratio L_1/L_2 to be 1) then the ratio of J_1/J_2 is determined by the ratio of the chemical potential differences $\Delta\mu_1/\Delta\mu_2$. This latter ratio can be altered by changing the kind of solvent and nonsolvent and by modifying solvent and nonsolvent proportions in film and bath. Wijmans et al.[25] changed the ratio of $\Delta\mu_1/\Delta\mu_2$ (and so J_1/J_2) by adding solvent to the coagulation bath. The coagulation path is then less steep and the binodal is intersected at much lower polymer concentrations (see Fig. 2, arrow AB). In this way it is even possible to obtain microporous membranes without dense top layers. Contrarily, in order to obtain a dense top layer it is necessary that the coagulation path should be as steep as possible.

Another factor which is important for the formation of a dense top layer is the location of the binodal. Altena and Smolders[23] were able to calculate numerically the location of the binodal of a ternary system using Flory–Huggins thermodynamics. They showed that the location of the binodal demixing gap primarily depends on the g_{12} and χ_{13} parameters. For a fixed value of χ_{13} (say 1.5) an increase in g_{12} (i.e., an increase in excess free energy of mixing between solvent and nonsolvent) will cause a shift of the binodal to a higher nonsolvent content [Fig. 4(a)]. For a fixed value of g_{12} (say 0.5) an increase in χ_{13} (i.e., decrease of polymer–nonsolvent interaction) will cause a shift of the binodal to a lower nonsolvent content [Fig. 4(b)]. For a very high value of χ_{13} (say 4.0) the binodal is located very near to the solvent–polymer axis, and an increase in g_{12} then hardly has any influence on the location of the binodal.

What is the influence of the location of the binodal on the compactness and density of the top layer? The more the binodal has been shifted to the polymer–nonsolvent axis, the more it is likely that the gel region is reached before the binodal will be intersected. This is schematically shown in Figure 5. In a sense this effect parallels the influence of another factor: the location of the gel region, since also when altering gelation (for instance, by temperature variation) one can monitor the conditions at the intersection of the demixing gap.

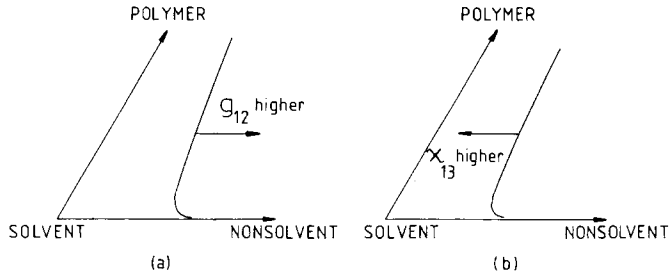

Fig. 4. Direction of the shift of the binodal: (a) increasing g_{12}, χ_{13} constant; (b) increasing χ_{13}, g_{12} constant.

In the experimental part we will focus our attention on two factors which influence the formation of a dense top layer strongly: polymer concentration; location of the binodal. The location of the gel region is still a rather unknown factor, and we have not further explored it here.

EXPERIMENTAL

Materials

Cellulose acetate (E 398-3) was obtained from Eastman Chemicals, polysulfone (P 3500) from Union Carbide, poly(2,6-dimethylphenyleneoxide) from General Electric and polyacrylonitrile (T 75) from DuPont. The solvents used were of analytical grade.

Membrane Preparation

Homogeneous Membranes. Polymer solutions were prepared by dissolving the polymer in a suitable solvent. Membranes were prepared by casting the polymer solution upon a glass plate after which the solvent was allowed to evaporate in a nitrogen atmosphere. The membranes obtained were completely transparant except for polyacrylonitrile.

Asymmetric Membranes. Asymmetric membranes were prepared by immersion precipitation. A polymer solution containing 10–30% by weight

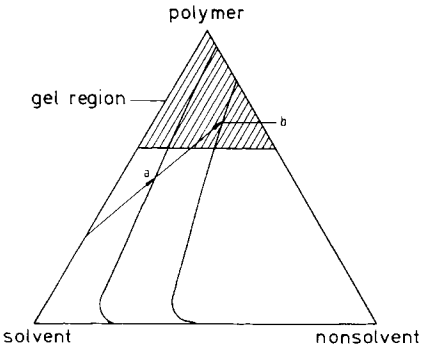

Fig. 5. Schematic course of a coagulation path reaching first the binodal (a) or the gel region (b), depending upon the binodal curve.

was cast upon a glass plate, and after immersion in a nonsolvent bath at room temperature the membrane was obtained.

Determination of the Phase Diagram

The location of the binodal in the phase diagram has been determined by titration. Solutions of solvent/nonsolvent were carefully added to polymer solutions at room temperature (20°C) until permanent turbidity (detected visually) was obtained. This indicated the boundary between the one-phase region and the two-phase region.

Pervaporation

The pervaporation experiments were carried out as described previously.[31] Vacuum at the downstream side was maintained at a pressure of 13.3 Pa (0.1 mm Hg) by a Crompton Parkinson vacuum pump. The pressure was measured by an Edwards piranhi gauge. The experiments were carried out for 8 h. A product sample was taken every hour and generally steady-state conditions were reached within about 3 h. The temperature of the liquid feed mixture was 20°C. The asymmetric membranes were installed with the top layer facing the feed.

Product Analysis

Analysis of binary ethanol–water mixtures was performed on a Varian model 3700 gaschromatograph fitted with a chromosorb 60/80 column and equipped with a thermal conductivity detector. For low ethanol concentrations (0–5 %) a flame ionization detector was used.

Scanning Electron Microscopy

Cross sections of the membranes were examined with a JEOL JSM 35 CF scanning electron microscope. Air-dried samples were prepared by cryogenic breaking followed by coating the sample with a charge conducting layer of gold by means of a Balzer union sputter unit.

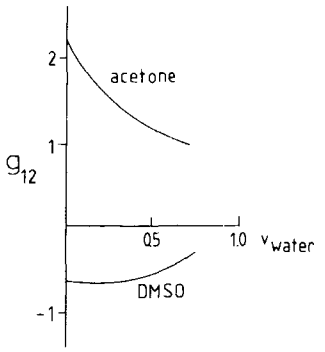

Fig. 6. Concentration dependent g_{12} parameters for the binary systems acetone/water and DMSO/water (from Ref. 23).

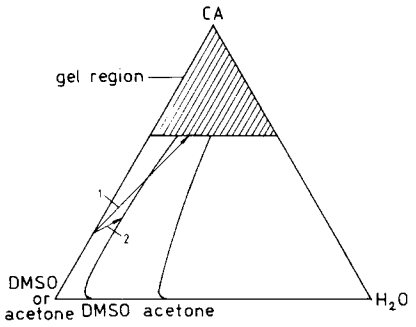

Fig. 7. Influence of the location of the liquid–liquid demixing gap and of the direction of the coagulation path on membrane formation. The location of the binodals are taken from Altena.[23] The location of the gel region is chosen arbitrarily: (1) DMSO as solvent; (2) acetone as solvent.

RESULTS AND DISCUSSION

In the first example to be treated here we will show the influence of the g_{12} interaction parameter on the location of the binodal and its effect on membrane performance. For this purpose we will compare the systems water/DMSO/cellulose acetate (CA) and water/acetone/cellulose acetate (CA). The interaction parameters are taken from Altena and Smolders[23] and Mulder et al.[32] The g_{12} parameters for both water/acetone and water/DMSO as a function of the volume fraction of water are given in Figure 6. If the g_{12} parameter is large (i.e., a high value for the excess free energy of mixing and a low mutual affinity), the binodal demixing gap is shifted to higher nonsolvent concentrations while for low g_{12} values (i.e., low or negative values for the free energy of mixing) the binodal is shifted to lower nonsolvent content. In Figure 7 the binodals for the two systems, taken from Altena and Smolders,[23] are given. Asymmetric membranes prepared from the two systems have been tested on ethanol–water mixtures, and the results are given in Table I. These results clearly show that solvent/nonsolvent interactions (i.e., location of the binodal) and polymer concentration have a large influence on membrane performance. A shift of the binodal to higher water contents (acetone/CA) and an increase of the polymer concentration result in membranes with higher selectivities.

A second phenomenon which has to be taken into account is the direction of the coagulation path, given by the ratio J_1/J_2. In the case of acetone as

TABLE I
Pervaporation Results of Asymmetric Cellulose Acetate Membranes[a]

Solvent	Nonsolvent	Polymer concn (%)	α	Wt % H_2O in permeate	Perm. rate (cm/h × 10^2)
Acetone	Water	25	12.3	92.5	2.7
Acetone	Water	18	5.9	85.5	4.2
DMSO	Water	25	1.0	50.0	32.5
DMSO	Water	18	—	—	—[b]

[a] Feed: ethanol–water 50–50% by weight; temperature = 20°C.
[b] Permeability too high.

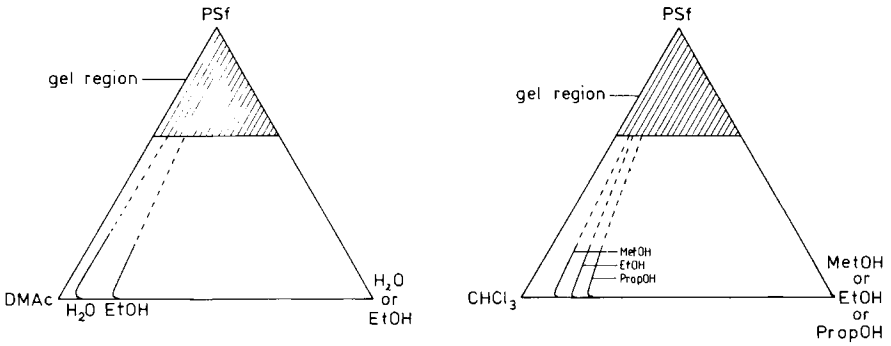

Fig. 8. Experimentally determined binodals for water/DMAc/PSf and ethanol/DMAc/PSf (a) and for methanol/$CHCl_3$/PSf, ethanol/$CHCl_3$/PSf, and propanol/$CHCl_3$/PSf (b).

solvent this ratio is much smaller in comparison with DMSO as solvent (see, for instance, Frommer and Lancet[33]).This results in a steep coagulation path and a more dense top layer (Fig. 7, arrow 1).

In the case of DMSO as solvent two effects cooperate to give a less dense top layer: The binodal is located near the solvent–polymer axis and the ratio J_1/J_2 is much higher giving a less steep coagulation path. Now the coagulation path can intersect the binodal in the neighbourhood of the gel region (Fig. 7, arrow 2) giving a membrane with a less compact top layer (membranes prepared from a 20% solution of CA in DMSO and water as nonsolvent have ultrafiltration properties[34]).

For systems with a very high χ_{13} value such as water (1)/polysulfone (3) the location of the binodal is almost completely determined by this parameter. By changing the kind of solvent in such a way that the mutual affinity between polymer and nonsolvent increases (χ_{13} decreases), the binodal will be shifted to higher nonsolvent content. In Figure 8(a) the experimental and calculated binodal for the system water/DMAc/polysulfone and the experimentally determined binodal for the system ethanol/DMAc/polysulfone are given. The experimentally determined binodals for the system methanol (respectively ethanol, propanol)/chloroform/polysulfone are given in Figure 8(b).

From these systems asymmetric membranes have also been prepared, and the pervaporation results are given in Table II. Again it is striking that selectively increases and permeation rate decreases if the binodal has

TABLE II
Pervaporation Results of Asymmetric Polysulfone Membranes[a]

Solvent	Nonsolvent	Polymer concn (%)	α	Wt % H_2O in permeate	Perm. rate (cm/h $\times$ 10^2)
DMAc	Water	15	—	—	—[b]
DMAc	Ethanol	15	1.0	50.0	7.0
$CHCl_3$	Methanol	15	8.3	89.2	0.2
$CHCl_3$	Ethanol	15	58	98.3	0.1
$CHCl_3$	Propanol	15	499	99.8	0.1

[a] Feed: ethanol–water 50–50% by weight; temperature = 20°C.
[b] Permeability too high.

TABLE III
Pervaporation Results of Asymmetric Polysulfone Membranes from the System *i*-Propanol/DMAc/Polysulfone[a]

Polymer concn (%)	α	Wt % H_2O in permeate	Perm. rate (cm/h $\times$ 10^2)
15	1.5	60.0	4.5
20	6.6	86.8	1.0
25	6.4	86.5	0.6
30	47	97.9	0.1
35	249	99.6	<0.1

[a] Feed: ethanol–water 50–50% by weight; temperature = 20°C.

been shifted to higher nonsolvent content. Another point to be noticed is that the location of the gel region will be affected by the nature of the nonsolvent used.

The last point to be considered is the influence of the polymer concentration on membrane performance. As was already demonstrated for cellulose acetate membranes, an increase in the polymer concentration of the polymer solution results in an increase in selectivity (see Table I). For the system *i*-propanol/DMAc/polysulfone we have varied the polymer concentration from 15 to 35% by weight of polymer and the results are given in Table III. From Table III one can see that the permeation rate decreases more than a factor 45 while the selectivity to ethanol/water mixtures increases from $\alpha = 1.5$ to $\alpha \sim 250$. Although the exact location of the binodal of this system has not been calculated (which is in fact not necessary for this qualitative explanation), the change of the coagulation is shown schematically in Figure 9. Going from 15 to 35% the coagulation path reaches the gel region at lower nonsolvent content. Cross sections of the asymmetric membranes from this system (*i*-propanol/DMAc/polysulfone with increasing polymer concentration from 15 to 35% by weight) are given in Figures 10–14. These figures clearly show that if the polymer concentration increases, the thickness of the top layer also increases. Recently Wijmans[35] showed that the thickness of the top layer of a polysulfone membrane (system: *i*-propanol/DMAc/polysulfone) can also be varied by changing the amount of solvent in the (nonsolvent) coagulation bath. The increase of the top layer thickness results in a decrease in permeation rate (see Table III).

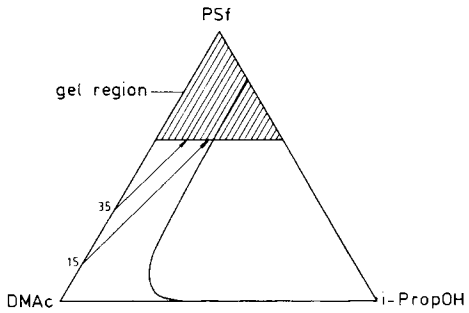

Fig. 9. Schematic course of the coagulation paths originating from different polymer concentrations for the system *i*-propanol/DMAc/PSf.

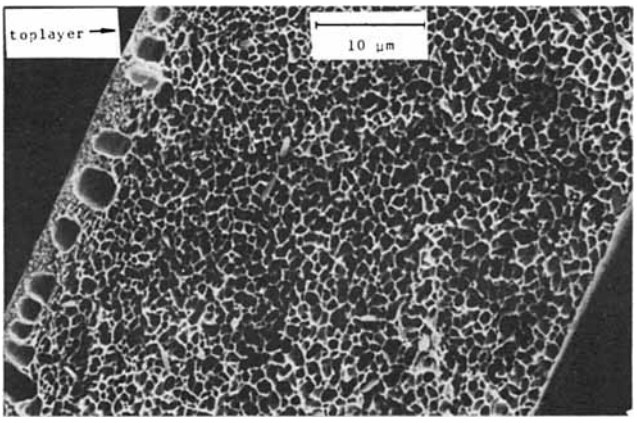

Fig. 10. Cross section of asymmetric membranes from the system *i*-propanol/DMAc/PSf: polymer concentration 15% by weight.

Generally, if the thickness of a homogeneous membrane increases, the permeation rate decreases roughly inversely proportional to membrane thickness while selectively is hardly affected.[1,36] However, if the results of Table III are considered, a very large increase in selectivity can be observed, and this cannot be explained by an increase in thickness of the top layer. Hence, the structure of the top layer will change and going from 15 to 35% a more dense and compact top layer is obtained. Furthermore, the resistance exerted by the sublayer will increase because the structure is changed from an open sponge (15% weight of polymer) to a closed cell (35% weight of polymer). A closed cell structure is not very desirable because the effective thickness of the membrane is not determined anymore by the thickness of the top layer.

The SEM photographs clearly support the hypothesis that two different types of phase separation are responsible for the formation of asymmetric membranes: gelation for the formation of the top layer and liquid–liquid

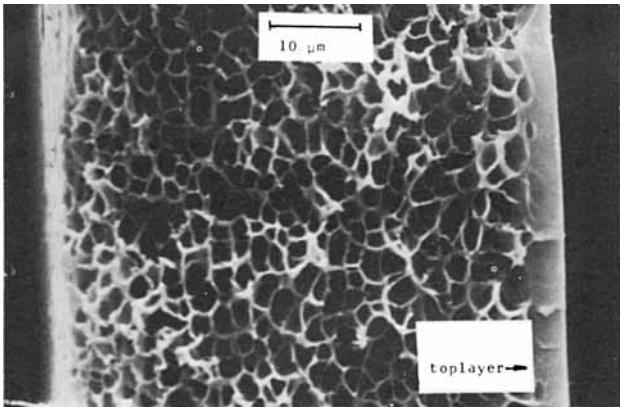

Fig. 11. Cross section of asymmetric membranes from the system *i*-propanol/DMAc/PSf: polymer concentration 20% by weight.

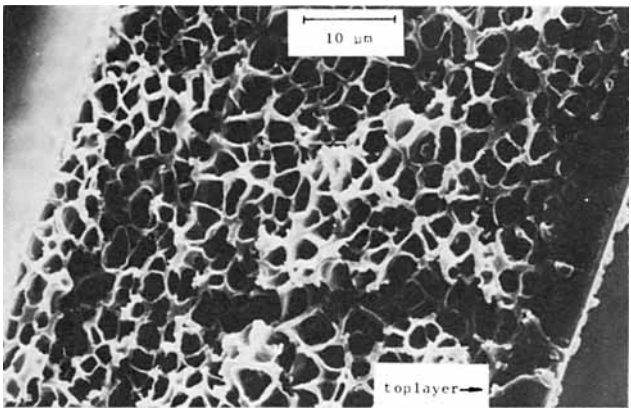

Fig. 12. Cross section of asymmetric membranes from the system *i*-propanol/DMAc/PSf: polymer concentration 25% by weight.

phase separation followed by gelation of the concentrated polymer phase for the formation of the porous sublayer.

Comparison of Homogeneous and Asymmetric Membranes

The objective of our investigations was to develop asymmetric pervaporation membranes in order to improve the permeability without loss in selectivity. Therefore, homogeneous membranes should be compared with the corresponding asymmetric membranes. The results are given in Table IV. One sees from Table IV that in all cases except for cellulose acetate an improvement in permeability was obtained.

The resistance to mass transfer of the asymmetric membranes is not only determined by the top layer but also to some extent by the sublayer. If this sublayer contains very small pores, the contribution to the total resistance can be considerable, and the advantage of a thin dense top layer as sole rate limiting factor does not hold anymore. Asymmetric CA membranes

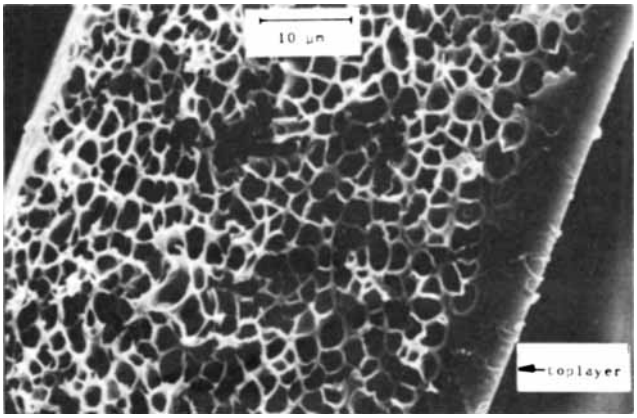

Fig. 13. Cross section of asymmetric membranes from the system *i*-propanol/DMAc/PSf: polymer concentration 30% by weight.

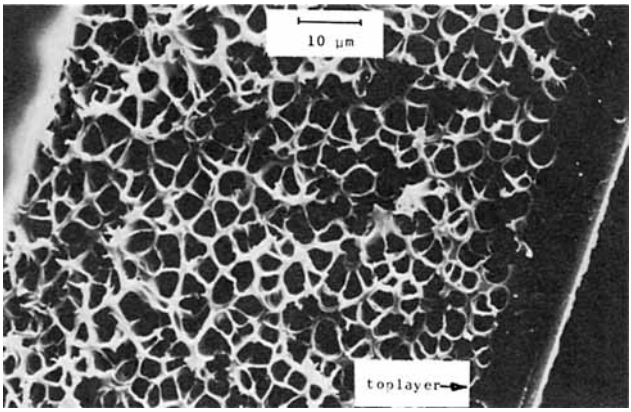

Fig. 14. Cross section of asymmetric membranes from the system *i*-propanol/DMAc/PSf: polymer concentration 35% by weight.

obtained from the system water/acetone/CA consist of a sublayer with very small pores (<0.1 µm), and therefore the permeation rate is not as large as expected. Moreover, the relatively low permeation rate can also be explained in part by the structure of the top layer: It has a more dense structure in comparison with the homogeneous membranes, as is indicated by the improved selectivity of the asymmetric CA membranes. The conclusion that small amounts of water increases the ordering of cellulose acetate gels resulting in a more compact structure is in agreement with differential scanning calorimetry measurements performed by Altena et al.[37] For the other polymers an improvement in permeation rate has been obtained; however, a small loss in selectivity can be observed.

CONCLUSIONS

In order to obtain asymmetric pervaporation membranes with a dense top layer different factors are important: polymer concentration (should be high), ratio J_1/J_2 (should be small) and the location of the binodal demixing region and the gel region. The general mechanism of membrane formation

TABLE IV
Homogeneous Membranes vs. Asymmetric Membranes[a]

	Homogeneous		Asymmetric	
Polymer	Wt % H_2O in permeate	Perm. rate (cm/h × 10^2)	Wt % H_2O in permeate	Perm. rate (cm/h × 10^2)
CA	80.7	6.8	95.0[b]	3.3
PSf	>99.5	0.04	>99.5[c]	0.1
PPO	95.7	0.09	94.1[d]	0.2
PAN	>99.5	0.15	97.9[e]	1.9

[a] Membrane thickness (for the homogeneous membranes) = 20 µm; feed, ethanol–water 50–50% by weight; temperature = 20°C.

[b] System water/acetone/cellulose acetate (CA).

[c] System propanol/$CHCl_3$/polysulfone (PSf).

[d] System ethanol/trichloroethylene/polyphenyleneoxide (PPO).

[e] System *i*-propanol/DMAc/polyacrylonitrile (PAN).

follows the scheme: top layer—gelation by entanglement (in the case of amorphous polymers); sublayer—liquid–liquid phase separation followed by gelation of the concentrated polymer phase. The SEM photographs clearly support the hypothesis that two different types of phase separation are responsible for the formation of asymmetric membranes. Asymmetric membranes have been prepared with high selectivities towards ethanol–water mixtures. In comparison with the homogeneous membranes the asymmetric membranes show higher permeabilities (as expected) while the selectivity remains the same or decreases slightly. Cellulose acetate is an exception because the asymmetric membranes show higher selectivities and lower permeation rates compared to the homogeneous membranes.

The highly selective asymmetric pervaporation membranes have, compared to asymmetric ultrafiltration and hyperfiltration membranes, relatively thick top layers. The thickness of the top layer can be varied by changing the polymer concentration or by adding solvent to the (nonsolvent) coagulation bath.

This paper is based upon work financially supported by the Ministeries van Economische Zaken en Onderwijs en Wetenschappen in The Netherlands. The authors thank Mr. C. Padberg for taking the SEM photographs.

References

1. R. C. Binning, R. J. Lee, J. F. Jennings, and E. C. Martin, *Ind. Eng. Chem.*, **53**, 45 (1961).
2. R. C. Binning and R. J. Lee, *Pet. Refiner*, **37**, 214 (1958).
3. R. C. Binning, R. J. Lee, J. F. Jennings, and E. C. Martin, *Am. Chem. Soc., Div. Pet. Chem. Prepr.*, **3**, 131 (1958).
4. M. H. V. Mulder, J. Oude Hendrikman, H. Hegeman, and C. A. Smolders, *J. Membr. Sci*, **16**, 269 (1983).
5. P. Aptel, J. Cuny, J. Jozefowicz, G. Morel, and J. Neel, *J. Appl. Polym. Sci.*, **16**, 106 (1972).
6. G. C. Tealdo, P. Canepa, and S. Munari, *J. Membr. Sci.*, **9**, 191 (1981).
7. R. Y. M. Huang and H. R. Jarvis, *J. Appl. Polym. Sci.*, **14**, 2341 (1970).
8. E. Nagy, D. Borlai, and A. Ujhidy, *J. Membr. Sci.*, **7**, 109 (1980).
9. K. C. Hoover and S. T. Hwang, *J. Membr. Sci.*, **10**, 253 (1982).
10. H. E. A. Brüschke, W. H. Schneider, and G. F. Tusel, lecture presented at the European Workshop on Pervaporation, September 21–22, 1982, Nancy, France; *Membrane News*, No. 4, 1983, published by the European Society of Membrane Science and Technology.
11. M. H. V. Mulder and C. A. Smolders, *J. Membr. Sci.*, **17**, 289 (1984).
12. D. R. Paul and J. D. Paciotti, *J. Polym. Sci., A-2*, **13**, 1201 (1975).
13. C. H. Lee, *J. Appl. Polym. Sci.*, **19**, 83 (1975).
14. F. W. Greenlaw, R. A. Shelden, and E. V. Thompson, *J. Membr. Sci.*, **2**, 333 (1977).
15. R. Rautenbach and R. Albrecht, lecture presented at the European Workshop on Pervaporation, September 21–22, 1982, Nancy, France.
16. S. Loeb and S. Sourirajan, *Adv. Chem. Ser.*, **38**, 117 (1962).
17. D. M. Koenhen, M. H. V. Mulder, and C. A. Smolders, *J. Appl. Polym. Sci.*, **21**, 199 (1977).
18. L. Broens, D. M. Koenhen, and C. A. Smolders, *Desalination*, **22**, 205 (1977).
19. L. Broens, F. W. Altena, C. A. Smolders, and D. M. Koenhen, *Desalination*, **32**, 33 (1980).
20. C. A. Smolders, in *Ultrafiltration Membranes and Application*, A. R. Cooper, Ed., Polym. Sci. Technol., **13**, Plenum, New York, 1980, p. 57.
21. F. W. Altena and C. A. Smolders, *J. Polym. Sci., Polym. Symp.*, **69**, 1 (1981).
22. H. Bokhorst, F. W. Altena, and C. A. Smolders, *Desalination*, **38**, 349 (1981).
23. F. W. Altena and C. A. Smolders, *Macromolecules*, **15**, 1491 (1982).
24. J. G. Wijmans and C. A. Smolders, in NATO ASI Series, Reidel, New York, in press.
25. J. G. Wijmans, J. P. B. Baay, and C. A. Smolders, *J. Membr. Sci.*, **14**, 263 (1983).
26. R. E. Kesting, *Synthetic Polymeric Membranes*, McGraw-Hill, New York, 1971, Chap. 5.

27. C. Cohen, G. B. Tanny, and S. Prager, *J. Polym. Sci., Polym. Phys. Ed.*, **17**, 477 (1979).
28. P. J. Flory, *Principles of Polymer Chemistry*, Cornell Univ. Press, Ithaca, NY, 1953.
29. A. Zivný and J. Pouchlý, *J. Polym. Sci., A-2*, **10**, 1467 (1972).
30. F. W. Altena, Ph.D. Thesis, Twente University of Technology, Enschede, The Netherlands, 1982, Chap. 7.
31. M. H. V. Mulder, F. Kruitz, and C. A. Smolders, *J. Membr. Sci.*, **11**, 349 (1982).
32. M. H. V. Mulder, T. Franken, and C. A. Smolders, *J. Membr. Sci.*, 22, 155 (1985).
33. M. A. Frommer and D. Lancet, in *Reverse Osmosis Membrane Research*, H. K. Lonsdale and H. E. Podall, Eds., Plenum, New York, 1972.
34. R. Bloch and M. A. Frommer, *Desalination*, **7**, 259 (1970).
35. J. G. Wijmans, R. J. Johanns, and C. A. Smolders, *J. Membr. Sci.*, to appear.
36. P. Aptel, J. Cuny, J. Jozefowicz, G. Morel, and J. Neel, *J. Appl. Polym. Sci.*, **18**, 351 (1974).
37. F. W. Altena, J. S. Schröder, R. v. d. Hulst, and C. A. Smolders, *J. Polym. Sci.*, Polym. Phys. Ed., in press.

Received May 1, 1984
Accepted October 22, 1984